

Distributionally Robust Weighted k -Nearest Neighbors

Shixiang Zhu, Liyan Xie, Minghe Zhang, Rui Gao, Yao Xie

Abstract

Learning a robust classifier from a few samples remains a key challenge in machine learning. A major thrust of research has been focused on developing k -nearest neighbor (k -NN) based algorithms combined with metric learning that captures similarities between samples. When the samples are limited, robustness is especially crucial to ensure the generalization capability of the classifier. In this paper, we study a minimax distributionally robust formulation of weighted k -nearest neighbors, which aims to find the optimal weighted k -NN classifiers that hedge against feature uncertainties. We develop an algorithm, Dr. k -NN, that efficiently solves this functional optimization problem and features in assigning minimax optimal weights to training samples when performing classification. These weights are class-dependent, and are determined by the similarities of sample features under the least favorable scenarios. When the size of the uncertainty set is properly tuned, the robust classifier has a smaller Lipschitz norm than the vanilla k -NN, and thus improves the generalization capability. We also couple our framework with neural-network-based feature embedding. We demonstrate the competitive performance of our algorithm compared to the state-of-the-art in the few-training-sample setting with various real-data experiments.

1 Introduction

Machine learning has been proven successful in data-intensive applications but is often hampered when the data set is small. For example, in breast mammography diagnosis for breast cancer screening [Aresta et al.(2019)Aresta, Araújo, Kwok, Chennamsetty, Safwan, Alex, Marami, Prastawa, Chan, Donovan, Fernandez, Zeineh, Kohl, Walz, Ludwig, Braunewell, Baust, Vu, To, Kim, Kwak, Galal, Sanchez-Freire, Brancati, Frucci, Riccio, Wang, Sun, Ma, Fang, Kone, Boulmane, Campilho, Eloy, Polónia, and Aguiar], the diagnosis of the type of breast cancer requires specialized analysis by pathologists in a highly time- and cost-consuming task and often leads to non-consensual results. As a result, labeled data in digital pathology are generally very scarce; so do many other applications.



Figure 1: Motivating example: a small training set of three image-label pairs: the first image is a mop; the second image is a dog; the third image looks like a mop but is, in fact, a dog (dressing up as a mop). The query (the last image) is “closer” to the third one and more likely to be misclassified as a dog if we use distance-weighted k -NN.

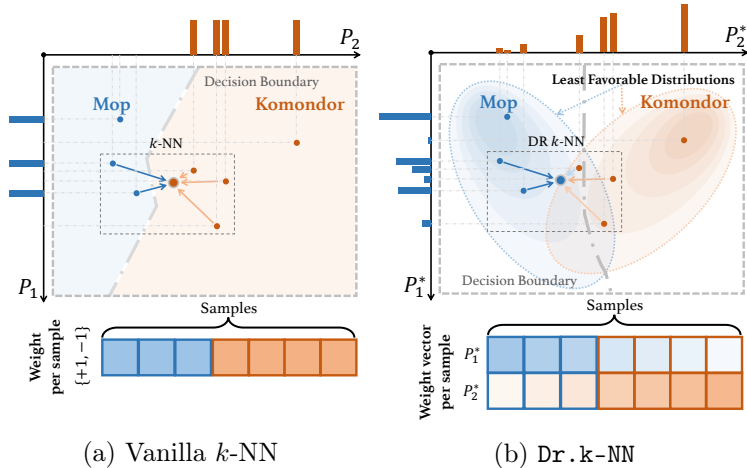


Figure 2: An illustrative comparison of Dr.k-NN and vanilla k -NN. Each colored dot is a training sample, where the color indicates its class-membership. The horizontal/vertical bar represents the probability mass of one training sample under the distribution P_1 , P_2 , respectively.

In this paper, we aim to tackle the general multi-class classification problem when only very few training samples are available for each class [Wang et al.(2019)Wang, Yao, Kwok, and Ni]. Evidently, k -Nearest Neighbor (k -NN) algorithm [Altman(1992)] is a natural idea to tackle this problem and shows promising empirical performances. Notable contributions, including seminal work [Goldberger et al.(2005)Goldberger, Hinton, Roweis, and Salakhutdinov] and the follow-up non-linear version [Salakhutdinov & Hinton(2007)Salakhutdinov and Hinton], go beyond the vanilla k -NN and propose neighborhood component analysis (NCA). NCA learns a distance metric that minimizes the expected leave-one-out classification error on the training data using a stochastic neighbor selection rule. Some recent studies in few-shot learning utilize the limited training data using a similar idea, such as matching network [Vinyals et al.(2016)Vinyals, Blundell, Lillicrap, Kavukcuoglu, and Wierstra] and prototypical network [Snell et al.(2017)Snell, Swersky, and Zemel]. They are primarily based on distance-weighted k -NN, which classifies an unseen sample (aka. *query*) by a weighted vote of its neighbors and uses the distance between two data points in the embedding space as their weights.

The classification performance of weighted k -NN critically depends on the choice of weighting scheme. The distance measuring the similarity between samples is typically chosen by metric learning, where a task-specific distance metric is automatically constructed from supervised data [Koch et al.(2015)Koch, Zemel, and Salakhutdinov, Plötz & Roth(2018)Plötz and Roth, Vinyals et al.(2016)Vinyals, Blundell, Lillicrap, Kavukcuoglu, and Wierstra]. However, it has been recognized that they may be not robust to the *few-training-samples* scenario, where an “outlier” may greatly deteriorate the performance. An example to illustrate this issue is shown in Figure 1. The training set with only three labeled samples includes two categories we want to classify: mop and Komondor. As we can see, the query image is visually closer to the third sample and thus more likely to be misclassified as a Komondor. Here the third sample in the training set is an “outlier”, since it is a Komondor dressing up as a mop, and it misleads the metric learning model to capture irrelevant details (e.g., the bucket and the mop handle) for the Komondor category. Such a problem can become even severe when the sample size is small.

The discussion above highlights the importance of choosing a good weighting scheme in weighted k -NN. To develop algorithms that are more robust in the few-training-samples settings, we propose

a new formulation of distributionally robust weighted k -nearest neighbors. More specifically, for a given set of features of training samples, we solve a Wasserstein distributionally robust optimization problem that finds the minimax optimal weight functions for the k -nearest neighbors. This infinite-dimensional functional optimization over weight functions presents a unique challenge for which existing literature on distributionally robust optimization do not consider. To tackle this challenge, we first consider a relaxed problem that optimizes over all randomized classifiers, which turns out to admit a finite-dimensional convex programming reformulation in spite of being infinite-dimensional (Theorem 1). Next, we show that there is a weighted k -NN classifier achieving the same risk and shares the same least favorable distributions (LFDs) as the robust classifier (Theorem 2). Thereby we prove the optimality of such weighted k -NN classifier for the original distributionally robust weighted k -nearest neighbors problem. Furthermore, we derive the generalization bound of the robust weighted k -NN classifier by relating it to a Lipschitz regularization problem (Theorem 3), and showing that its Lipschitz norm can be smaller than the vanilla k -NN classifier and thus has a better control on the generalization gap (Corollary 1).

Based on these theoretical results, we proposed a novel algorithm called **Dr.k-NN**. Unlike the traditional distance-weighted k -NN that uses the same weight for all label classes, our algorithm introduces a vector of weights, one for each class, for each sample in k -NN and performs a weighted majority vote. These weights are determined from the LFDs and reveal the significance of each sample in the worst case, thereby contributing effectively to final decision making. An example is illustrated in Figure 2. Further, using differentiable optimization [Amos & Kolter(2017)Amos and Kolter, Agrawal et al.(2019)Agrawal, Amos, Barratt, Boyd, Diamond, and Kolter], we incorporate a neural network into the minimax classifier that jointly learns the feature embedding and the minimax optimal classifier. Numerical experiments show that our algorithm can effectively improve the multi-class classification performance with few training samples on various data sets.

Related work Recently, there has been much interest in multi-class classification with few training samples, see [Wang et al.(2019)Wang, Yao, Kwok, and Ni] for a survey. The main idea of our work is related to metric learning [Plötz & Roth(2018)Plötz and Roth, Goldberger et al.(2005)Goldberger, Hinton, Roweis, and Salakhutdinov, Salakhutdinov & Hinton(2007)Salakhutdinov and Hinton], which essentially translates the hidden information carried by the limited data into a distance metric, and has been widely adopted in few-shot learning and meta learning [Finn et al.(2017)Finn, Abbeel, and Levine, Koch et al.(2015)Koch, Zemel, and Salakhutdinov, Snell et al.(2017)Snell, Swersky, and Zemel, Vinyals et al.(2016)Vinyals, Blundell, Lillicrap, Kavukcuoglu, and Wierstra, Li et al.(2006)Li, Fergus, and Perona]. However, unlike few-shot and meta learning, where the goal is to acquire meta knowledge from a large number of observed classes and then predict examples from unobserved classes, we focus on attacking a specific general classification problem where the number of categories is fixed but labeled data are scarce. In this paper, we take a different probabilistic approach to exploit information from the data: we construct an uncertainty set for distributions of each class based on the Wasserstein distance.

Wasserstein distributionally robust optimization [Esfahani & Kuhn(2018)Esfahani and Kuhn, Abadeh et al.(2015)Abadeh, Esfahani, and Kuhn, Blanchet & Murthy(2019)Blanchet and Murthy, Gao & Kleywegt(2016)Gao and Kleywegt, Sinha et al.(2017)Sinha, Namkoong, and Duchi, Blanchet et al.(2019)Blanchet, Kang, and Murthy, Shafieezadeh-Abadeh et al.(2019)Shafieezadeh-Abadeh, Kuhn, and Esfahani, Gao et al.(2017)Gao, Chen, and Kleywegt] is an emerging paradigm for statistical learning; see [Kuhn et al.(2019)Kuhn, Esfahani, Nguyen, and Shafieezadeh-Abadeh] for a recent survey. Our work is mostly related to [Gao et al.(2018)Gao, Xie, Xie, and Xu], a framework for Wasserstein robust hypothesis testing, but is different in three important ways. First,

we focus on multi-class classification, while [Gao et al.(2018)Gao, Xie, Xie, and Xu] only studied two hypotheses. Second, we focus on directly minimizing the mis-classification error while [Gao et al.(2018)Gao, Xie, Xie, and Xu] used a convex relaxation for the 0-1 loss. Third, we analyze the generalization bound while [Gao et al.(2018)Gao, Xie, Xie, and Xu] does not. Fourth, while [Gao et al.(2018)Gao, Xie, Xie, and Xu] requires sample features as an input, we develop a scalable algorithmic framework to simultaneously learn the optimal feature extractor parameterized by neural networks and robust classifier to achieve the best performance. A recent work [Chen & Paschalidis(2019)Chen and Paschalidis] studies distributionally robust k -NN regression. Note that regression and classification are fundamentally different as different performance metrics are used. In [Chen & Paschalidis(2019)Chen and Paschalidis] the objective is to minimize the mean square error, whereas in our work we minimize classification errors. Another well-known work on optimal weighted nearest neighbor binary classifier [Samworth(2012)] assigns one weight to each sample; the optimal weights minimize asymptotic expansion for the excess risk (regret). In contrast, we consider minimax robust multi-class classification, each training sample is associated with different weights for different classes.

2 Distributionally Robust k -NN

In this section, we present our model. We first define weighted k -NN classifier in Section 2.1, then present the proposed framework of distributionally robust k -NN problem in Section 2.2.

2.1 Weighted k -NN classifier

Let $\{(x^1, y^1), \dots, (x^n, y^n)\}$ be a set of training samples, where x^i denotes the i -th data sample in the observation space \mathcal{X} , and $y^i \in \mathcal{Y} := \{1, \dots, M\}$ denotes the class (label) of the i -th data sample. Let $\phi : \mathcal{X} \rightarrow \Xi$ be a feature extractor that embeds samples to the feature space Ξ (in Section 4.2 we will train a neural network to learn ϕ). Denote the sample feature vectors and the empirical support as:

$$\xi^i := \phi(x^i), \quad i = 1, \dots, n, \quad \hat{\Xi} := \{\xi^1, \dots, \xi^n\}.$$

Let

$$S = \{(\xi^1, y^1), \dots, (\xi^n, y^n)\}.$$

Define empirical distributions:

$$\hat{P}_m := \frac{1}{|\{i : y^i = m\}|} \sum_{i=1}^n \delta_{\xi^i} \mathbb{I}\{y^i = m\}, \quad m = 1, \dots, M,$$

where δ denotes the Dirac point mass, $|\cdot|$ denotes the cardinality of a set, and \mathbb{I} denotes the indicator function.

Let $\pi : \Xi \rightarrow \Delta_M$ be a *randomized* classifier that assigns class $m \in \{1, \dots, M\}$ with probability $\pi_m(\xi)$ to a query feature vector $\xi \in \Xi$, where Δ_M is the probabilistic simplex $\Delta_M = \{\pi \in \mathbb{R}_+^M : \sum_{m=1}^M \pi_m = 1\}$. It is worth mentioning that the randomized test is more general than the commonly seen deterministic test. In particular, the random classifier π reduces to the deterministic test if for any ξ , there exists a m such that $\pi_m(\xi) = 1$. Suppose the features in each class m follows a distribution P_m . We define the *risk* of a classifier π as the total error probabilities¹

$$\Psi(\pi; P_1, \dots, P_M) := \sum_{m=1}^M \mathbb{E}_{\xi \sim P_m} [1 - \pi_m(\xi)]. \quad (1)$$

¹To ease the exposition we consider only equal weights over the error probabilities, but our results can be easily generalized to any weighted average of error probabilities.

Recall that the vanilla k -NN is performed as follows. Let $c : \Xi \times \Xi \rightarrow \mathbb{R}_+$ be a metric on Ξ that measures distance between features. For any given query point ξ , let $\tau_1^S(\xi), \dots, \tau_n^S(\xi)$ be a reordering of $\{1, \dots, n\}$ according to their distance to ξ , i.e., $c(\xi, \xi^{\tau_i^S(\xi)}) \leq c(\xi, \xi^{\tau_{i+1}^S(\xi)})$ for all $i < n$, where the tie is broken arbitrarily. Here the superscript S indicates the dependence on the sample S . In vanilla k -NN, we compute the votes as

$$p_m(\xi) := \sum_{i=1}^k \frac{1}{k} \mathbb{I}\{y^{\tau_i^S(\xi)} = m\}, \quad m = 1, \dots, M. \quad (2)$$

The vanilla k -NN decides the class for ξ by the majority vote, i.e., accept the class $\arg \max_{1 \leq m \leq M} p_m(\xi)$.

To define a weighted k -NN, let us replace the equal weights in (2) by an arbitrary weight function $w_m : \Xi \times \Xi \rightarrow \mathbb{R}_+$ for each class $m = 1, \dots, M$:

$$p_m(\xi) := \sum_{i=1}^k w_m(\xi, \xi^{\tau_i^S(\xi)}), \quad (3)$$

and use a shorthand notation $w := (w_1, \dots, w_M)$. In the sequel, we define a general tie-breaking rule as follows. For any ξ , denote $\mathcal{M}_0(\xi) := \arg \max_{1 \leq m \leq M} p_m(\xi)$. When $|\mathcal{M}_0(\xi)| > 1$, there is a tie at ξ . We denote $\pi_m(\xi)$ as the probability of accepting class m for $m \in \mathcal{M}_0(\xi)$ and we have $\sum_{m \in \mathcal{M}_0(\xi)} \pi_m(\xi) = 1$.

We define a *weighted k -NN classifier* $\pi^{\text{knn}}(\xi; k, w) : \Xi \rightarrow \Delta_M$ as:

$$\pi_m^{\text{knn}}(\xi; k, w) = \begin{cases} \pi_m(\xi), & m \in \mathcal{M}_0(\xi), \\ 0, & \text{otherwise.} \end{cases} \quad (4)$$

A weighted k -NN classifier involves two parameters: number of nearest neighbors k and weighting scheme w . Particularly, $w_m(\xi, \xi^i) = \mathbb{I}\{y^i = m\}$ recovers the vanilla k -NN, and $w_m(\xi, \xi^i) = \mathbb{I}\{y^i = m\}/c(\xi, \xi^i)$ recovers the distance-based weighted k -NN. Note that our definition (3) allows different weighting schemes for different classes, which is more general than the standard weighted k -NN.

The goal is to find the optimal weighted k -NN classifier $\pi^{\text{knn}}(\cdot; k, w)$ such that the risk Ψ as defined in (1) is minimized. Since the underlying true distributions are unknown, the commonly used loss function is the empirical loss, i.e., substitute the empirical distributions \hat{P}_m into the risk function (1). This leads to the following optimization problem:

$$\min_{\substack{1 \leq k \leq n \\ w_m : \Xi \times \Xi \rightarrow \mathbb{R}_+, 1 \leq m \leq M}} \Psi(\pi^{\text{knn}}(\cdot; k, w); \hat{P}_1, \dots, \hat{P}_M). \quad (5)$$

It is worth mentioning that this minimization problem is an *infinite-dimensional* functional optimization, since the weighting schemes w is a function on $\Xi \times \Xi$.

2.2 Distributionally robust k -NN

For few-training-sample setting, the empirical distributions might not be good estimates for the true distribution since the sample size is small. To hedge against distributional uncertainty, we propose a distributionally robust counterpart of the weighted k -NN problem defined in the previous subsection. Specifically, suppose each class m is associated with a distributional uncertainty set \mathcal{P}_m , which will be specified shortly. Given $\mathcal{P}_1, \dots, \mathcal{P}_M$, define the *worst-case risk* of a classifier π as the worst-case total error probabilities

$$\max_{P_m \in \mathcal{P}_m, 1 \leq m \leq M} \Psi(\pi; P_1, \dots, P_M),$$

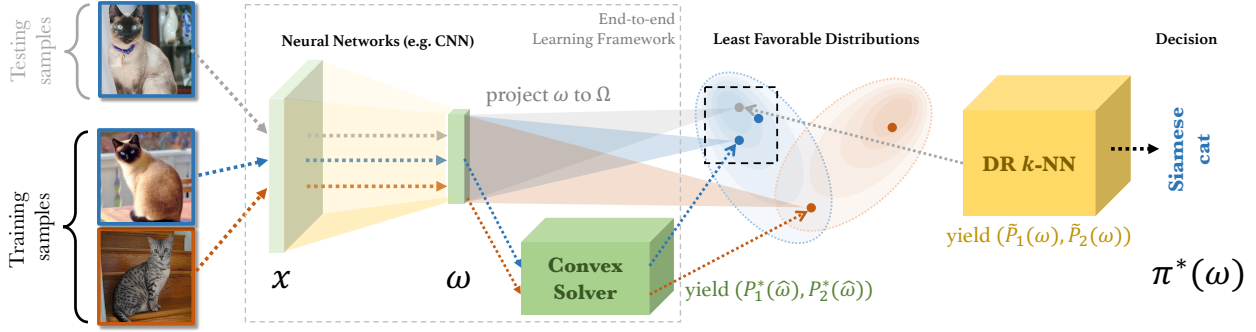


Figure 3: An overview of the end-to-end learning framework, which consists of two cohesive components: (1) an architecture that is able to produce feature embedding ξ and least favorable distributions P_m^* for training set; (2) an Dr.k-NN makes decisions for any unseen sample ξ based on the estimated weight vector $\tilde{p}_m(\xi)$ (probability mass on least favorable distributions).

where Ψ is defined in (1).

We consider the following distributionally robust k -NN problem that finds the optimal weighted k -NN classifier minimizing the worst-case risk:

$$\min_{\substack{1 \leq k \leq n \\ w_m: \Xi \times \Xi \rightarrow \mathbb{R}_+ \\ 1 \leq m \leq M}} \max_{\substack{P_m \in \mathcal{P}_m \\ 1 \leq m \leq M}} \Psi(\pi^{\text{knn}}(\cdot; k, w); P_1, \dots, P_M). \quad (6)$$

Here the optimal solution P_1^*, \dots, P_M^* to the inner maximization problem is also called *least favorable distributions (LFD)* in statistics literature [Huber(1965)]. We summarize the architecture of the proposed distributionally robust k -NN framework in Figure 3, more details are provided in Section 4.

Now we describe the uncertainty set \mathcal{P}_m . First, since we are going to re-weight the training samples to build the classifier, we restrict the support of every distribution in \mathcal{P}_m to $\hat{\Xi}$, the set of empirical points. Second, the uncertainty set is data-driven, containing the empirical distribution \hat{P}_m and distributions surrounding its neighborhood. Third, to measure the closeness between distributions, we choose the Wasserstein metric of order 1 [Villani(2008)], defined as

$$\mathcal{W}(P, P') := \min_{\gamma} \mathbb{E}_{(\xi, \xi') \sim \gamma} [c(\xi, \xi')]$$

for any two distributions P and P' on Ξ , where the minimization of γ is taken over the set of all probability distributions on $\Xi \times \Xi$ with marginals P and P' . The main advantage of using Wasserstein metric is that it takes account of the *geometry* of the feature space by incorporating the metric $c(\cdot, \cdot)$ in its definition. Given the empirical distribution \hat{P}_m for $m = 1, \dots, M$, we define

$$\mathcal{P}_m := \{P_m \in \mathcal{P}(\hat{\Xi}) : \mathcal{W}(P_m, \hat{P}_m) \leq \vartheta_m\}, \quad (7)$$

where $\mathcal{P}(\hat{\Xi})$ denotes the set of all probability distributions on $\hat{\Xi}$; $\vartheta_m \geq 0$ specifies the size of the uncertainty set for the m -th class that specifies the amount of deviation we would like to control.

3 Theoretical Properties

In this section, we analyze the computational tractability and statistical properties of the proposed distributionally robust weighted k -NN classifier found in (6). All proofs are delegated to Appendix A.

3.1 Robust Classification

Observe that similar to (5), the formulation (6) is also an infinite-dimensional functional optimization. Let us first relate it to a relaxed robust classification problem, which turns out to be more tractable.

Consider the following minimax robust classification problem over all randomized classifiers π (recalling Δ_M is the probability simplex in \mathbb{R}_+^M):

$$\min_{\pi: \Xi \rightarrow \Delta_M} \max_{P_m \in \mathcal{P}_{m,1} \leq m \leq M} \Psi(\pi; P_1, \dots, P_M). \quad (8)$$

Yet still, (8) is an infinite-dimensional functional optimization, since we are optimizing over the set of all randomized classifiers. We establish the following theorem stating a finite-dimensional convex programming reformulation for the problem (8).

Theorem 1. *For the uncertainty sets defined in (7), the least favorable distribution of problem (8) can be obtained by solving the following problem:*

$$\begin{aligned} & \min_{\substack{p_1, \dots, p_M \in \mathbb{R}_+^n \\ \gamma_1, \dots, \gamma_M \in \mathbb{R}_+^{n \times n}}} \sum_{i=1}^n \max_{1 \leq m \leq M} p_m^i \\ & \text{subject to} \quad \sum_{i=1}^n \sum_{j=1}^n \gamma_m^{i,j} c(\xi^i, \xi^j) \leq \vartheta_m, \\ & \quad \sum_{i=1}^n \gamma_m^{i,j} = \widehat{P}_m(\xi^j), \quad \sum_{j=1}^n \gamma_m^{i,j} = p_m^i, \\ & \quad \forall 1 \leq i, j \leq N, \quad 1 \leq m \leq M. \end{aligned} \quad (9)$$

The decision variable $\gamma_m \in \mathbb{R}_+^{n \times n}$ can be viewed as a joint distribution on n empirical points with marginal distributions \widehat{P}_m and P_m , represented by a vector $p_m \in \mathbb{R}_+^n$. The inequality constraint controls the Wasserstein distance between P_m and \widehat{P}_m .

Below we give an intuitive explanation for the objective function in (9). Note that $\max_{1 \leq m' \leq M} p_{m'}^i - p_m^i$ measures the margin between the maximum likelihood of ξ^i among all classes and the likelihood of the m -th class. Thus, the objective in (9) can be equivalently rewritten as minimization of total margin:

$$\sum_{i=1}^n \sum_{m=1}^M \left(\max_{1 \leq m' \leq M} p_{m'}^i - p_m^i \right).$$

When $M = 2$, the total margin reduces to the total variation distance. Also, let $y_m^i \in \{0, 1\}$ be the class indicator variable of sample ξ^i , observe that

$$\sum_{i=1}^n \max_{1 \leq m \leq M} p_m^i = \lim_{t \rightarrow \infty} \left(\sum_{i=1}^n \sum_{m=1}^M y_m^i p_m^i - \frac{1}{t} \sum_{i=1}^n \sum_{m=1}^M y_m^i \log \frac{\exp(tp_m^i)}{\sum_{m=1}^M \exp(tp_m^i)} \right),$$

where the second term on the right side represents the cross-entropy (or negative log-likelihood).

Therefore, problem (9) perturbs $(\widehat{P}_1, \dots, \widehat{P}_M)$ to LFDs (P_1^*, \dots, P_M^*) so as to minimize the total margin as well as an upper bound on cross-entropy of LFDs; the smaller the margin (or cross-entropy) is, the more similar between classes and thus the harder to distinguish among them.

3.2 Expressiveness of Weighted k -NN

In this subsection we study the expressive power of the class of weighted k -NN classifiers

$$\{\pi^{\text{knn}}(\cdot; k, w): 1 \leq k \leq n, w_m: \Xi \times \Xi \rightarrow \mathbb{R}_+, 1 \leq m \leq M\}$$

defined in Section 2.1.

The following theorem establishes the equivalence between the original problem (6) and the relaxed robust classification problem (8) studied in Section 3.1.

Theorem 2. *For the uncertainty set defined in (7), formulations (6) and (8) have identical optimal values. In addition, there exists optimal solutions of (6) and (8) that share common LFDs that are optimal to (9).*

Theorem 2 implies that the set of weighted k -NN classifiers is *exhaustive*, in the sense that it achieves the same optimal robust risk as optimizing over the set of all randomized classifiers. In our proof, we show that the *weighted 1-NN classifier*, with weights equal to the LFDs of (9), is an optimal solution to (6). Therefore, instead of solving (6) directly, by Theorem 1, we can solve the convex program (9) for the LFDs, based on which we construct a robust k -NN classifier. This justifies the Dr.k-NN algorithm to be described in Section 4.

3.3 Lipschitz Regularization and Generalization Bound

Next, we discuss the generalization bound – measured by the population risk under the true distribution – of the proposed distributional robust k -NN framework, by relating (6) and (8) to Lipschitz regularization.

Using duality for Wasserstein DRO [Gao & Kleywegt(2016)Gao and Kleywegt], problem (8) is equivalent to

$$\min_{\substack{\pi: \hat{\Xi} \rightarrow \Delta_M \\ \lambda_m \geq 0, m=1, \dots, M}} \left\{ \sum_{m=1}^M \lambda_m \vartheta_m + \mathbb{E}_{\xi \sim \hat{P}_m} \left[\max_{\xi \in \hat{\Xi}} \left\{ 1 - \pi_m(\xi) - \lambda_m c(\xi, \hat{\xi}) \right\} \right] \right\}. \quad (10)$$

Then by [Gao et al.(2017)Gao, Chen, and Kleywegt], this problem is upper bounded by the following Lipschitz regularized classification problem

$$\min_{\pi: \hat{\Xi} \rightarrow \Delta_M} \sum_{m=1}^M \left\{ \mathbb{E}_{\xi \sim \hat{P}_m} [1 - \pi_m(\xi)] + \vartheta_m \|\pi_m\|_{\text{Lip}} \right\}, \quad (11)$$

where $\|\pi_m\|_{\text{Lip}} := \max_{\xi, \tilde{\xi} \in \hat{\Xi}, \xi \neq \tilde{\xi}} \frac{|\pi_m(\tilde{\xi}) - \pi_m(\xi)|}{c(\tilde{\xi}, \xi)}$ is the Lipschitz norm of the function π_m for each $m = 1, \dots, M$. Perhaps surprisingly, the next result shows that (10) and (11) are actually equivalent (thus by Theorem 2, are both equivalent to (6)), despite that the loss function does not satisfy existing criteria ensuring the equivalence [Esfahani & Kuhn(2018)Esfahani and Kuhn, Shafieezadeh-Abadeh et al.(2019)Shafieezadeh-Abadeh, Kuhn, and Esfahani, Gao et al.(2017)Gao, Chen, and Kleywegt].

Theorem 3. *Formulations (10) and (11) are equivalent, and there exists an optimizer π^* of (11) satisfying $\|\pi_m^*\|_{\text{Lip}} = \lambda_m^*$, $m = 1, \dots, M$, where $(\lambda_m^*)_m$ is the optimizer of (10) when $\pi = \pi^*$.*

The theorem is proved by using c -transform [Villani(2008)] to show that any optimizer π_m^* can be modified into a λ_m^* -Lipschitz classifier while maintaining the optimality. An immediate consequence of Theorem 3 based on is the following generalization bound of (6).

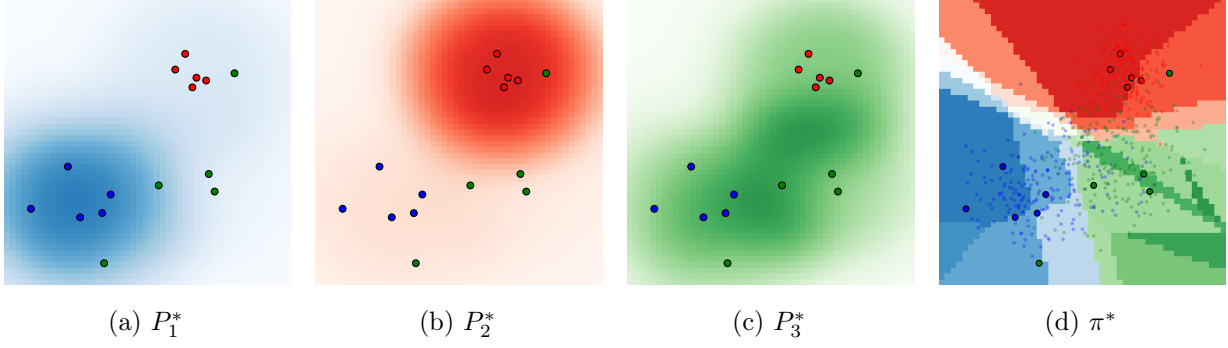


Figure 4: An example of the weights P_1^*, P_2^*, P_3^* yielding from (9) and the corresponding results of Dr.k-NN using a small subset of MNIST (digit 4 (red), 6 (blue), 9 (green) and $k = 5$). Raw samples are projected on a 2D feature space ($d = 2$), with the color indicating their true class-membership. In (a)(b)(c), shaded areas indicate the kernel smoothing of P_1^*, P_2^*, P_3^* defined in (13). In (d), big dots represent the training points and small dots represent the query points, and their color depth suggests how likely the sample is being classified into the true category.

Corollary 1. *There exists an optimal robust 1-NN classifier $\pi^{\text{knn}}(\cdot; 1, w^*)$ with generalization gap controlled by $\frac{1}{\min_{1 \leq m \leq M} \vartheta_m} \cdot \mathfrak{R}_n(\text{Lip}(\Xi))$, where $\mathfrak{R}_n(\text{Lip}(\Xi))$ is the Rademacher complexity of the 1-Lipschitz functions on Ξ .*

In comparison, the margin-based generalization gap of the vanilla 1-NN classifier for binary classification is controlled by $\frac{2}{d(\widehat{\Xi}_1, \widehat{\Xi}_2)} \cdot \mathfrak{R}_n(\text{Lip}(\Xi))$, where $\widehat{\Xi}^m := \{\xi^i : y^i = m\}$ is the set of samples in the m -th class [von Luxburg & Bousquet(2004) von Luxburg and Bousquet]. Therefore, the generalization gap of the distributionally robust 1-NN classifier can be smaller than that of the vanilla 1-NN classifier by tuning the radii $(\vartheta_m)_m$ properly.

4 Proposed Algorithm Dr.k-NN

In this section, we present the Distributional robust k -Nearest Neighbor (Dr.k-NN) algorithm, which is a direct consequence of the theoretical justifications in Section 3.

4.1 Dr.k-NN algorithm

Based on Theorem 2, our algorithm contains two steps.

Step 1. [Sample re-weighting] For each class m , re-weight n samples using a distribution P_m^* , where (P_1^*, \dots, P_M^*) is the p -component of the minimizer of (9).

Step 2. [k -NN] Given a query point ξ , ordering the training samples according to their distance to ξ : $c(\xi, \xi^{\tau_1^S(\xi)}) \leq c(\xi, \xi^{\tau_2^S(\xi)}) \leq \dots \leq c(\xi, \xi^{\tau_n^S(\xi)})$. Compute the weighted k -NN votes, define

$$\tilde{p}_m(\xi) := \frac{1}{k} \sum_{i=1}^k P_m^*(\xi^{\tau_i^S(\xi)}), \quad m = 1, \dots, M. \quad (12)$$

Decide the class for a query feature point ξ as $\arg \max_{1 \leq m \leq M} \tilde{p}_m(\xi)$, where the tie is broken according to the rule (4).

Figure 4 gives an illustration showing the probabilistic weights (P_1^*, P_2^*, P_3^*) for three classes and its corresponding decision boundary yielding from the weighted k -NN.

Algorithm 1 Learning algorithm for Dr.k-NN

Input: $S_m := \{(x^i, y^i) : y^i = m, \forall i\} \subset S, m = 1, \dots, M$;

Output: The feature mapping $\phi(\cdot; \theta)$ and the LFD P_1^*, \dots, P_M^* supported on training samples;

Initialization: θ_0 is randomly initialized; $n' < n$ is the size of “mini-set”; $t = 0$;

while $t < T$ **do**

for *number of mini-sets* **do**

 Randomly generate M integers n_1, \dots, n_M such that $\sum_{m=1}^M n_m = n', n_m > 0, \forall m$;

 Initialize two ordered sets $\widehat{\Xi} = \emptyset, \widehat{P} = \emptyset$;

for $m \in \{1, \dots, M\}$ **do**

$\mathcal{X}_m \leftarrow$ Randomly sample n_m points from S_m ;

$\widehat{\Xi}_m \leftarrow \{\xi := \phi(x; \theta_t) : x \in \mathcal{X}_m\}$;

$\widehat{P}_m \leftarrow \frac{1}{n_m} \sum_{i=1}^{n_m} \delta_{\xi_m^i}, \xi_m^i \in \widehat{\Xi}_m$;

$\widehat{\Xi} \leftarrow \widehat{\Xi} \cup \widehat{\Xi}_m; \widehat{P} \leftarrow \widehat{P} \cup \widehat{P}_m$;

end

 Update the probability mass of LFDs P_1^*, \dots, P_M^* on $\widehat{\Xi}$ by solving (9) given $\widehat{\Xi}, \widehat{P}$;

end

$\theta_{t+1} \leftarrow \theta_t - \alpha \nabla J(\theta_t; P_1^*, \dots, P_M^*)$, where α is the learning rate;

$t \leftarrow t + 1$;

end

For the sake of completeness, we also extend our algorithm to non-few-training-sample setting, which is referred to as truncated Dr.k-NN. The key idea is to keep the training samples that are important in deciding the decision boundary based on the maximum entropy principle [Cover & Thomas(2006)Cover and Thomas]. This can be particularly useful for the general classification problem with an arbitrary size of training set. An illustration (Figure 6) and more details can be found in Appendix B.

4.2 Joint learning framework

In this section, we propose a framework that jointly learns the feature mapping and the robust classifier. Let the feature mapping $\phi(\cdot; \theta)$ be a neural network parameterized by θ whose input is a batch of training samples (Figure 3), and then compose it with an optimization layer that packs the convex problem (9) as an output layer that outputs the LFDs of (8). The optimization layer is adopted from differentiable optimization [Amos & Kolter(2017)Amos and Kolter, Agrawal et al.(2019)Agrawal, Amos, Barratt, Boyd, Diamond, and Kolter], in which the optimization problem is integrated as an individual layer in an end-to-end trainable deep networks and the solution of the problem can be backpropagated through neural networks.

To apply the mini-batch stochastic gradient descent, we need to ensure that each batch comprises of multiple “mini-sets”, one for each class, containing at least one training sample from each class fed into the convex optimization layer. In light of (9), the objective of our joint learning framework is $\min_{\theta} J(\theta; P_1^*, \dots, P_M^*)$, where

$$J(\theta; P_1^*, \dots, P_M^*) := \sum_{i=1}^n \max_{1 \leq m \leq M} P_m^*(\phi(x^i; \theta)),$$

and $\{P_m^*(\phi(\cdot; \theta))\}_{1 \leq m \leq M}$ are the LFDs generated by the convex solver defined in (9) given input variables $\{\xi^i = \phi(x^i; \theta)\}_{1 \leq i \leq n}$. The algorithm is summarized in Algorithm 1.

Table 1: Comparison of classification accuracy in the few-training-sample setting

Methods	MNIST				mini ImageNet				CIFAR-10				Omniglot				Lung Cancer		COVID-19 CT	
	$M=2$		$M=5$		$M=2$		$M=5$		$M=2$		$M=5$		$M=2$		$M=5$		$M=3$		$M=2$	
	$K=5$	$K=10$	$K=5$	$K=10$	$K=5$	$K=10$	$K=5$	$K=10$	$K=5$	$K=10$	$K=5$	$K=10$	$K=5$	$K=10$	$K=5$	$K=10$	$K=5$	$K=8$	$K=5$	$K=10$
PCA+k-NN	0.801	0.872	0.614	0.678	0.578	0.667	0.268	0.277	0.687	0.711	0.262	0.270	0.597	0.638	0.309	0.358	0.617	0.647	0.658	0.719
SVD+k-NN	0.749	0.790	0.524	0.567	0.587	0.675	0.268	0.283	0.680	0.701	0.259	0.266	0.591	0.618	0.305	0.413	0.624	0.648	0.646	0.715
NCA+k-NN	0.602	0.640	0.340	0.355	0.547	0.578	0.245	0.258	0.597	0.616	0.232	0.236	0.549	0.574	0.267	0.346	0.575	0.582	0.612	0.624
Matching Net	0.732	0.830	0.625	0.732	0.687	0.703	0.286	0.360	0.632	0.641	0.241	0.247	0.735	0.769	0.412	0.433	0.621	0.635	0.715	0.732
Prototypical Net	0.742	0.842	0.671	0.759	0.710	0.725	0.296	0.348	0.651	0.664	0.254	0.259	0.769	0.836	0.448	0.532	0.632	0.644	0.729	0.744
MetaOptNet	0.725	0.843	0.658	0.790	0.732	0.741	0.255	0.363	0.702	0.713	0.257	0.298	0.742	0.755	0.412	0.453	0.638	0.642	0.713	0.739
Feature embedding + k-NN	0.792	0.798	0.546	0.551	0.738	0.742	0.490	0.486	0.689	0.691	0.492	0.494	0.725	0.751	0.445	0.495	0.664	0.691	0.701	0.710
Kernel Smoothing	0.777	0.873	0.559	0.579	0.593	0.601	0.272	0.278	0.642	0.661	0.272	0.282	0.520	0.565	0.240	0.285	0.367	0.370	0.582	0.604
Truncated Dr.k-NN	0.815	0.926	0.742	0.825	0.746	0.753	0.295	0.340	0.703	0.719	0.297	0.305	0.755	0.825	0.425	0.542	0.652	0.693	0.722	0.741
Dr.k-NN	0.838	0.959	0.746	0.831	0.752	0.786	0.306	0.358	0.707	0.728	0.309	0.311	0.765	0.850	0.465	0.580	0.667	0.704	0.734	0.752

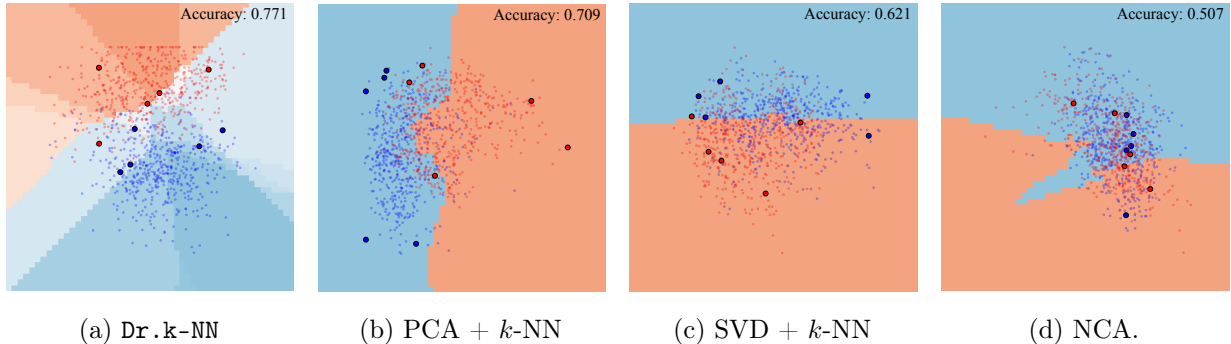


Figure 5: A comparison of the learned feature spaces and the corresponding decision boundaries. There are 10 training samples from two categories of MNIST identified as large dots and 1,000 query samples identified as small dots. The color of dots shows their true categories. The color of the region shows the decisions made by corresponding methods.

5 Experiments

In this section, we evaluate our method and eight alternative approaches on four commonly-used image data sets: MNIST [LeCun & Cortes(2010)LeCun and Cortes], CIFAR-10 [Krizhevsky et al.(2020)Krizhevsky, Nair, and Hinton], Omniglot [Lake et al.(2015)Lake, Salakhutdinov, and Tenenbaum], and present a set of comprehensive numerical examples.

We also test our method on two medical diagnosis data sets: Lung Cancer [Dua & Graff(2017)Dua and Graff], and COVID-19 CT [Yang et al.(2020)Yang, He, Zhao, Zhang, Zhang, and Xie], where very few data samples are available for study, due to privacy concerns and high costs associated with harvesting data. Specifically, Lung Cancer data record 56 attributes for only 32 patients who have been diagnosed with three types of pathological lung cancers; COVID-19 Computed Tomography (CT) data contain 349 COVID-19 CT images from 216 patients and 463 non-COVID-19 CTs. Here, we present a few examples of COVID-19 CT images and non-COVID-19 CT images in Appendix D.

Experiment set-up. We compare our method including Dr.k-NN and its truncated version with the following baselines: (1) k -NN based methods with different dimension reduction techniques, including Principal Component Analysis (PCA+k-NN), Singular Value Decomposition (SVD+k-NN), Neighbourhood Components Analysis (NCA+k-NN) [Goldberger et al.(2005)Goldberger, Hinton, Roweis, and Salakhutdinov], and feature embeddings generated by Dr.k-NN (Feature embedding + k -NN) as a sanity check; (2) matching networks [Vinyals et al.(2016)Vinyals, Blundell, Lillicrap, Kavukcuoglu, and Wierstra]; (3) prototypical networks [Snell et al.(2017)Snell, Swersky, and Zemel]; (4) MetaOptNet [Lee et al.(2019)Lee, Maji, Ravichandran, and Soatto]. To make these methods comparable, we adopt the same naive neural network with a single CNN layer on matching network, prototypical

network, and our model, respectively, where the kernel size is 3, the stride is 1 and the width of the output layer is $d = 400$.

In our experiments, we focus on an M -class K -sample (K training samples for each class) learning task. To generate the training data set, we randomly select M classes and for each class we take K random samples. So our training data set contains MK samples overall. We then aim to classify a disjoint batch of unseen samples into one of these M classes. Thus random performance on this task stands at $1/M$. We test the average performance of different methods using 1,000 unseen samples from the same M classes. To obtain reliable results, we repeat each test 10 times and calculate the average accuracy.

Other experimental configurations are described as follows: The Adam optimizer [Kingma & Ba(2014)Kingma and Ba] is adopted for all experiments conducted in this paper, where learning rate is 10^{-2} . The mini-batch size is 32. The hyper-parameter ϑ_m is chosen by cross-validation, which varies from application to application. The differentiable convex optimization layer we adopt is from [Agrawal et al.(2019)Agrawal, Amos, Barratt, Boyd, Diamond, and Kolter]. To make all approaches comparable, we use the same network structure in matching network, prototypical network, and MetaOptNet as we described above. We use the Euclidean distance $c(\xi, \xi') = \|\xi - \xi'\|_2$ throughout our experiment. All experiments are performed on Google Colaboratory (Pro version) with 12GB RAM and dual-core Intel processors, which speed up to 2.3 GHz (without GPU).

Results. We present the average test accuracy in Table 1 for the unseen samples with different $M = 2, 5$ and $K = 5, 10$ on small subsets of MNIST, *mini* ImageNet, CIFAR-10, Omniglot, and with $M = 3$ and $K = 5, 8$ on lung cancer data. Note that random performance for two-class and five-class classifications are 0.5 and 0.2, respectively. The figures in Table 1 show that **Dr.k-NN** ($k = 5$) outperforms other baselines in terms of the average test accuracy on all data sets. We note that 95% confidence interval of our method’s performance on all the data sets is smaller than 0.08. The truncated **Dr.k-NN** also yields competitive results using only 20% training samples ($\tau = 0.9$), compared to standard **Dr.k-NN**.

To confirm that the proposed learning framework will affect the distribution of hidden representation of data points, we show the training and query samples in a 2D feature space and the corresponding decision boundary in Figure 5. It turns out our framework finds a better feature representation in the 2D space with a smooth decision boundary and a reasonable decision confidence map (indicated by the color depth in Figure 5 (a)).

Comparison to kernel smoothing. We also compare with an approach using kernel-smoothing of the LFDs (in contrast to using k -NN) for performing classification. Consider a Gaussian kernel $\kappa(x) = |H_h|^{-1/2} \kappa(H_h^{-1/2} x)$, where $H_h = hI_p$ is the isotropical kernel with bandwidth h . Then we replace $\tilde{p}_m(\xi)$ in Step 2 of **Dr.k-NN** with the following

$$\tilde{p}_m(\xi) := \sum_{i=1}^n P_m^*(\xi^i) \kappa(\xi - \xi^i), \quad \forall \xi, \quad m = 1, \dots, M. \quad (13)$$

We evaluate both methods on a subset of MNIST, which contains 1,000 testing samples (small dots) and 20 training samples (large dots) from two categories (indexed by blue and red, respectively).

As shown in Figure 7 and Figure 8 (Appendix C), our experimental results have shown the importance of using k -NN in our proposed algorithm, where the **Dr.kNN** significantly outperforms the parallel version using kernel smoothing (even after the kernel bandwidth being optimized). We find that the performance when using kernel smoothing (13) heavily depends on selecting an appropriate kernel bandwidth h as illustrated by Figure 8.

Moreover, the best kernel bandwidth may vary from one dataset to another. Therefore, the cross-validation is required to be carried out to find the best kernel bandwidth in practice, which is quite time-consuming. In contrast, choosing the hyper-parameter k is an easy task, since we only have limited choices of k in few-training-sample scenario and the performance of Dr.k-NN is insensitive to the choices of k (see Figure 7).

6 Conclusion

We propose a distributionally robust k -NN classifier (Dr.k-NN) for tackling the multi-class classification problem with few training samples. To make a decision, each neighboring sample is weighted according to least favorable distributions resulting from a distributionally robust problem. As shown in the theoretical results and demonstrated by experiments, our methods achieve outstanding performance in classification accuracy compared with other baselines using minimal resources. The robust classifier layer (9) serves an alternative to the usual softmax layer in a neural network for classification, and we believe it is promising for other machine learning tasks.

References

- [Abadeh et al.(2015)Abadeh, Esfahani, and Kuhn] Abadeh, S. S., Esfahani, P. M. M., and Kuhn, D. Distributionally robust logistic regression. In *Advances in Neural Information Processing Systems*, pp. 1576–1584, 2015.
- [Agrawal et al.(2019)Agrawal, Amos, Barratt, Boyd, Diamond, and Kolter] Agrawal, A., Amos, B., Barratt, S., Boyd, S., Diamond, S., and Kolter, J. Z. Differentiable convex optimization layers. In *Advances in Neural Information Processing Systems*, pp. 9558–9570, 2019.
- [Altman(1992)] Altman, N. S. An introduction to kernel and nearest-neighbor nonparametric regression. *The American Statistician*, 46(3):175–185, 1992. doi: 10.1080/00031305.1992.10475879.
- [Amos & Kolter(2017)Amos and Kolter] Amos, B. and Kolter, J. Z. Optnet: Differentiable optimization as a layer in neural networks. In *Proceedings of the 34th International Conference on Machine Learning-Volume 70*, pp. 136–145. JMLR. org, 2017.
- [Aresta et al.(2019)Aresta, Araújo, Kwok, Chennamsetty, Safwan, Alex, Marami, Prastawa, Chan, Donovan, Fernandez, G., Zeineh, J., Kohl, M., Walz, C., Ludwig, F., Braunewell, S., Baust, M., Vu, Q. D., To, M. N. N., Kim, E., Kwak, J. T., Galal, S., Sanchez-Freire, V., Brancati, N., Frucci, M., Riccio, D., Wang, Y., Sun, L., Ma, K., Fang, J., Kone, I., Boulmane, L., Campilho, A., Eloy, C., Polónia, A., and Aguiar, P. Bach: Grand challenge on breast cancer histology images. *Medical Image Analysis*, 56:122 – 139, 2019. ISSN 1361-8415. doi: <https://doi.org/10.1016/j.media.2019.05.010>.
- [Blanchet & Murthy(2019)Blanchet and Murthy] Blanchet, J. and Murthy, K. Quantifying distributional model risk via optimal transport. *Mathematics of Operations Research*, 44(2):565–600, 2019.
- [Blanchet et al.(2019)Blanchet, Kang, and Murthy] Blanchet, J., Kang, Y., and Murthy, K. Robust Wasserstein profile inference and applications to machine learning. *Journal of Applied Probability*, 56(3):830–857, 2019.

- [Chen & Paschalidis(2019)Chen and Paschalidis] Chen, R. and Paschalidis, I. Selecting optimal decisions via distributionally robust nearest-neighbor regression. In Wallach, H., Larochelle, H., Beygelzimer, A., dAlché Buc, F., Fox, E., and Garnett, R. (eds.), *Advances in Neural Information Processing Systems 32*, pp. 749–759. Curran Associates, Inc., 2019.
- [Cover & Thomas(2006)Cover and Thomas] Cover, T. M. and Thomas, J. A. *Elements of Information Theory (Wiley Series in Telecommunications and Signal Processing)*. Wiley-Interscience, USA, 2006. ISBN 0471241954.
- [Dua & Graff(2017)Dua and Graff] Dua, D. and Graff, C. UCI machine learning repository: Lung cancer data set, 2017.
- [Esfahani & Kuhn(2018)Esfahani and Kuhn] Esfahani, P. M. and Kuhn, D. Data-driven distributionally robust optimization using the Wasserstein metric: Performance guarantees and tractable reformulations. *Mathematical Programming*, 171(1-2):115–166, 2018.
- [Finn et al.(2017)Finn, Abbeel, and Levine] Finn, C., Abbeel, P., and Levine, S. Model-agnostic meta-learning for fast adaptation of deep networks. In Precup, D. and Teh, Y. W. (eds.), *Proceedings of the 34th International Conference on Machine Learning*, volume 70 of *Proceedings of Machine Learning Research*, pp. 1126–1135, International Convention Centre, Sydney, Australia, 06–11 Aug 2017. PMLR.
- [Gao & Kleywegt(2016)Gao and Kleywegt] Gao, R. and Kleywegt, A. J. Distributionally robust stochastic optimization with Wasserstein distance. *arXiv preprint arXiv:1604.02199*, 2016.
- [Gao et al.(2017)Gao, Chen, and Kleywegt] Gao, R., Chen, X., and Kleywegt, A. J. Wasserstein distributional robustness and regularization in statistical learning. *arXiv preprint arXiv:1712.06050*, 2017.
- [Gao et al.(2018)Gao, Xie, Xie, and Xu] Gao, R., Xie, L., Xie, Y., and Xu, H. Robust hypothesis testing using Wasserstein uncertainty sets. In *Proceedings of the 32nd International Conference on Neural Information Processing Systems, NIPS’18*, pp. 7913–7923, Red Hook, NY, USA, 2018. Curran Associates Inc.
- [Goldberger et al.(2005)Goldberger, Hinton, Roweis, and Salakhutdinov] Goldberger, J., Hinton, G. E., Roweis, S. T., and Salakhutdinov, R. R. Neighbourhood components analysis. In Saul, L. K., Weiss, Y., and Bottou, L. (eds.), *Advances in Neural Information Processing Systems 17*, pp. 513–520. MIT Press, 2005.
- [Huber(1965)] Huber, P. J. A robust version of the probability ratio test. *Annals of Mathematical Statistics*, 36(6):1753–1758, 1965.
- [Kingma & Ba(2014)Kingma and Ba] Kingma, D. P. and Ba, J. Adam: A method for stochastic optimization. *arXiv preprint arXiv:1412.6980*, 2014.
- [Koch et al.(2015)Koch, Zemel, and Salakhutdinov] Koch, G., Zemel, R., and Salakhutdinov, R. Siamese neural networks for one-shot image recognition. In *ICML deep learning workshop*, volume 2. Lille, 2015.
- [Krizhevsky et al.(2020)Krizhevsky, Nair, and Hinton] Krizhevsky, A., Nair, V., and Hinton, G. Cifar-10 (canadian institute for advanced research). 2020.

- [Kuhn et al.(2019)Kuhn, Esfahani, Nguyen, and Shafieezadeh-Abadeh] Kuhn, D., Esfahani, P. M., Nguyen, V. A., and Shafieezadeh-Abadeh, S. Wasserstein distributionally robust optimization: Theory and applications in machine learning. In *Operations Research & Management Science in the Age of Analytics*, pp. 130–166. INFORMS, 2019.
- [Lake et al.(2015)Lake, Salakhutdinov, and Tenenbaum] Lake, B. M., Salakhutdinov, R., and Tenenbaum, J. B. Human-level concept learning through probabilistic program induction. *Science*, 350(6266):1332–1338, 2015.
- [LeCun & Cortes(2010)LeCun and Cortes] LeCun, Y. and Cortes, C. MNIST handwritten digit database. 2010.
- [Lee et al.(2019)Lee, Maji, Ravichandran, and Soatto] Lee, K., Maji, S., Ravichandran, A., and Soatto, S. Meta-learning with differentiable convex optimization. In *Proceedings of the IEEE Conference on Computer Vision and Pattern Recognition*, pp. 10657–10665, 2019.
- [Li et al.(2006)Li, Fergus, and Perona] Li, F., Fergus, R., and Perona, P. One-shot learning of object categories. *IEEE Transactions on Pattern Analysis and Machine Intelligence*, 28(4):594–611, 2006.
- [Plötz & Roth(2018)Plötz and Roth] Plötz, T. and Roth, S. Neural nearest neighbors networks. In *Proceedings of the 32nd International Conference on Neural Information Processing Systems, NIPS’18*, pp. 1095–1106, Red Hook, NY, USA, 2018. Curran Associates Inc.
- [Salakhutdinov & Hinton(2007)Salakhutdinov and Hinton] Salakhutdinov, R. and Hinton, G. Learning a nonlinear embedding by preserving class neighbourhood structure. In Meila, M. and Shen, X. (eds.), *Proceedings of the Eleventh International Conference on Artificial Intelligence and Statistics*, volume 2 of *Proceedings of Machine Learning Research*, pp. 412–419, San Juan, Puerto Rico, 21–24 Mar 2007. PMLR.
- [Samworth(2012)] Samworth, R. J. Optimal weighted nearest neighbour classifiers. *The Annals of Statistics*, 40(5):2733–2763, 2012.
- [Shafieezadeh-Abadeh et al.(2019)Shafieezadeh-Abadeh, Kuhn, and Esfahani] Shafieezadeh-Abadeh, S., Kuhn, D., and Esfahani, P. M. Regularization via mass transportation. *Journal of Machine Learning Research*, 20(103):1–68, 2019.
- [Shapiro et al.(2014)Shapiro, Dentcheva, and Ruszczyński] Shapiro, A., Dentcheva, D., and Ruszczyński, A. *Lectures on stochastic programming: modeling and theory*. SIAM, 2014.
- [Sinha et al.(2017)Sinha, Namkoong, and Duchi] Sinha, A., Namkoong, H., and Duchi, J. Certifying some distributional robustness with principled adversarial training. *arXiv preprint arXiv:1710.10571*, 2017.
- [Snell et al.(2017)Snell, Swersky, and Zemel] Snell, J., Swersky, K., and Zemel, R. Prototypical networks for few-shot learning. In Guyon, I., Luxburg, U. V., Bengio, S., Wallach, H., Fergus, R., Vishwanathan, S., and Garnett, R. (eds.), *Advances in Neural Information Processing Systems 30*, pp. 4077–4087. Curran Associates, Inc., 2017.
- [Villani(2008)] Villani, C. *Optimal transport: old and new*, volume 338. Springer Science & Business Media, 2008.

- [Vinyals et al.(2016)Vinyals, Blundell, Lillicrap, Kavukcuoglu, and Wierstra] Vinyals, O., Blundell, C., Lillicrap, T., Kavukcuoglu, K., and Wierstra, D. Matching networks for one shot learning. In *Proceedings of the 30th International Conference on Neural Information Processing Systems*, NIPS'16, pp. 3637–3645, Red Hook, NY, USA, 2016. Curran Associates Inc. ISBN 9781510838819.
- [von Luxburg & Bousquet(2004)von Luxburg and Bousquet] von Luxburg, U. and Bousquet, O. Distance-based classification with lipschitz functions. *J. Mach. Learn. Res.*, 5(Jun):669–695, 2004.
- [Wang et al.(2019)Wang, Yao, Kwok, and Ni] Wang, Y., Yao, Q., Kwok, J., and Ni, L. M. Generalizing from a few examples: A survey on few-shot learning, 2019.
- [Yang et al.(2020)Yang, He, Zhao, Zhang, Zhang, and Xie] Yang, X., He, X., Zhao, J., Zhang, Y., Zhang, S., and Xie, P. COVID-CT-Dataset: A CT scan dataset about COVID-19, 2020.

A Proofs for Section 3

A.1 Proof of Theorem 1

The proof of Theorem 1 is based on the following two lemmas.

Lemma 1. Fix probability distributions $P_1, \dots, P_M \in \mathcal{P}(\widehat{\Xi})$, where $\widehat{\Xi} = \{\xi^1, \dots, \xi^n\}$. Then

$$\psi(P_1, \dots, P_M) := \min_{\pi: \widehat{\Xi} \rightarrow \Delta_M} \Psi(\pi; P_1, \dots, P_M) = M - \sum_{i=1}^n \max_{1 \leq m \leq M} P_m(\xi^i).$$

Furthermore, the optimal classifier π^* satisfies that for any $\xi^i \in \widehat{\Xi}$,

$$\{m : \pi_m^*(\xi^i) > 0, 1 \leq m \leq M\} \subset \arg \max_{1 \leq m \leq M} \frac{P_m(\xi^i)}{\sum_{m=1}^M P_m(\xi^i)}.$$

This lemma gives a closed-form expression for the risk of the optimal classifier if P_1, \dots, P_M are known, and shows that the optimal decision π^* accepts the class with the maximum likelihood. Moreover, when there is a tie (i.e., the set $\arg \max_{1 \leq m \leq M} P_m(\xi)$ is not singleton), the optimal decision π^* can break the tie arbitrarily.

Proof of Lemma 1. We here prove a more general result for an arbitrary sample space Ξ . Note that each P_m , $1 \leq m \leq M$, is absolutely continuous with respect to $P_1 + \dots + P_M$, hence the Radon-Nikodym derivative $\frac{dP_m}{d(P_1 + \dots + P_M)}$ exists. Using the interchangeability principle [Shapiro et al.(2014)Shapiro, Dentcheva, and Ruszczyński] that enables us to exchange the minimization and integration, we have

$$\begin{aligned} \min_{\pi: \Xi \rightarrow \Delta_M} \Psi(\pi; P_1, \dots, P_M) &= \min_{\pi: \Xi \rightarrow \Delta_M} \int_{\Xi} \left[\sum_{m=1}^M (1 - \pi_m(\xi)) \frac{dP_m}{d(P_1 + \dots + P_M)}(\xi) \right] d(P_1 + \dots + P_M) \\ &= \int_{\Xi} \min_{\pi \in \Delta_M} \left[\sum_{m=1}^M (1 - \pi_m) \frac{dP_m}{d(P_1 + \dots + P_M)}(\xi) \right] d(P_1 + \dots + P_M) \\ &= \int_{\Xi} \left[1 - \max_{1 \leq m \leq M} \frac{dP_m}{d(P_1 + \dots + P_M)}(\xi) \right] d(P_1 + \dots + P_M), \end{aligned} \quad (14)$$

where the first equality is obtained by plugging in the definition of Ψ in (1); the second equality is due the interchangeability principle; and the last equality holds because for any ξ , the inner minimization attains its minimum at one of the vertices of Δ_M . More specifically, note that for each ξ , the objective of the inner minimization problem equals to $1 - \sum_{m=1}^M \pi_m \frac{dP_m}{d(P_1 + \dots + P_M)}(\xi)$. Under the constraint that $\pi \in \Delta_M$, i.e., $\sum_{m=1}^M \pi_m = 1$, we have:

$$\sum_{m=1}^M \pi_m \frac{dP_m}{d(P_1 + \dots + P_M)}(\xi) \leq \max_{1 \leq m \leq M} \frac{dP_m}{d(P_1 + \dots + P_M)}(\xi),$$

and the equality holds when π are chosen such that

$$\{m : \pi_m > 0, 1 \leq m \leq M\} \subset \arg \max_{1 \leq m \leq M} \frac{dP_m(\xi)}{\sum_{m=1}^M dP_m(\xi)}.$$

If there is a single maximum in $\{\frac{dP_m}{d(P_1 + \dots + P_M)}(\xi), 1 \leq m \leq M\}$, say at index m^* , then this simply implies that the optimal π is chosen as $\pi_{m^*} = 1$ and $\pi_m = 0$ for $m \neq m^*$.

If we substitute Ξ with the empirical support $\widehat{\Xi}$, the above formulation in Equation (14) translates into

$$\min_{\pi: \widehat{\Xi} \rightarrow \Delta_M} \Psi(\pi; P_1, \dots, P_M) = M - \sum_{i=1}^n \max_{1 \leq m \leq M} P_m(\xi^i),$$

therefore the lemma is proved. \square

Lemma 2. *For the uncertainty sets defined in (7), the problem $\max_{P_m \in \mathcal{P}_m, 1 \leq m \leq M} \psi(P_1, \dots, P_M)$ is equivalent to (9).*

Proof of Lemma 2. Recall that the Wasserstein metric of order 1 is defined as

$$\mathcal{W}(P, P') := \min_{\gamma} \mathbb{E}_{(\xi, \xi') \sim \gamma} [c(\xi, \xi')]$$

for any two distributions P and P' on Ξ , where the minimization of γ is taken over the set of all probability distributions on $\Xi \times \Xi$ with marginals P and P' , i.e., the set

$$\left\{ \gamma \in \mathcal{P}(\Xi \times \Xi) : \int_{\Xi} \gamma(\xi, \xi') d\xi' = P(\xi), \int_{\Xi} \gamma(\xi, \xi') d\xi = P'(\xi'), \forall \xi, \xi' \in \Xi \right\},$$

where $\mathcal{P}(\Xi \times \Xi)$ denotes the joint probability distributions on $\Xi \times \Xi$. Therefore, the Wasserstein metric $\mathcal{W}(P, P')$ can be rewritten as

$$\min_{\gamma} \left\{ \int_{\Xi \times \Xi} c(\xi, \xi') \gamma(\xi, \xi') d\xi d\xi' : \int_{\Xi} \gamma(\xi, \xi') d\xi' = P(\xi), \int_{\Xi} \gamma(\xi, \xi') d\xi = P'(\xi'), \forall \xi, \xi' \in \Xi \right\}$$

By the definition of uncertainty sets in (7) which contains discrete distributions supported on $\widehat{\Xi}$, we can introduce additional variables $\gamma_m \in \mathbb{R}_+^{n \times n}$ which represents the distribution on $\widehat{\Xi} \times \widehat{\Xi}$, with marginals $P_m \in \mathcal{P}_m$ and \widehat{P}_m , for $1 \leq m \leq M$. For any $\xi^i, \xi^j \in \widehat{\Xi}$, let $\gamma_m^{i,j}$ denotes $\gamma_m(\xi^i, \xi^j)$ for simplicity. Thus the objective function in the above reformulation of $\mathcal{W}(P_m, \widehat{P}_m)$ is $\sum_{i=1}^n \sum_{j=1}^n \gamma_m^{i,j} c(\xi^i, \xi^j)$. The constraints $\mathcal{W}(P_m, \widehat{P}_m) \leq \vartheta_m$ in (7) can be rewritten using γ_m as

$$\sum_{i=1}^n \sum_{j=1}^n \gamma_m^{i,j} c(\xi^i, \xi^j) \leq \vartheta_m, \quad m = 1, \dots, M.$$

Furthermore, the marginal distribution constraint of γ_m reads:

$$\sum_{i=1}^n \gamma_m^{i,j} = \widehat{P}_m(\xi^j), \quad \sum_{j=1}^n \gamma_m^{i,j} = P_m(\xi^i), \quad m = 1, \dots, M.$$

Thereby the problem $\max_{P_m \in \mathcal{P}_m, 1 \leq m \leq M} \psi(P_1, \dots, P_M)$ is equivalent to the convex optimization formulation in (9). \square

Proof to Theorem 1. By Lemmas 1 and 2, we have

$$\max_{P_m \in \mathcal{P}_m, 1 \leq m \leq M} \min_{\pi: \widehat{\Xi} \rightarrow \Delta_M} \Psi(\pi; P_1, \dots, P_M) = \max_{P_m \in \mathcal{P}_m, 1 \leq m \leq M} \psi(P_1, \dots, P_M) = (9).$$

To prove Theorem 1, it remains to verify the validity of exchanging max and min. We identify π as (π^1, \dots, π^n) , where $\pi^i \in \mathbb{R}_+^M$ satisfies $\sum_{m=1}^M \pi_m^i = 1$. Similar to the proof of Lemma 2, P_m , $1 \leq m \leq M$, can also be identified as a vector in \mathbb{R}^n . Note that the objective function $\Psi(\pi; P_1, \dots, P_M)$ is linear in (π^1, \dots, π^n) and concave in (P_1, \dots, P_M) , and the Slater condition holds. Hence applying convex programming duality we can exchange max and min and thus the result follows. It is worth mentioning that the optimal solution π^* and corresponding LFDs P_1^*, \dots, P_M^* always exist since they are solutions to a saddle point problem. \square

A.2 Proof of Theorem 2

Proof of Theorem 2. On the one hand, since $\pi^{\text{knn}}(\cdot; k, w)$ can be regarded as a special case of the general classifier $\pi : \Xi \rightarrow \Delta_M$, it holds that

$$\begin{aligned} & \min_{\substack{w_m: \Xi \times \Xi \rightarrow \mathbb{R}_+, \\ 1 \leq k \leq n}} \max_{P_m \in \mathcal{P}_m, 1 \leq m \leq M} \sum_{m=1}^M \mathbb{E}_{\xi_m \sim P_m} [1 - \pi_m^{\text{knn}}(\xi_m; k, w)] \\ & \geq \min_{\pi: \widehat{\Xi} \rightarrow \Delta_M} \max_{P_m \in \mathcal{P}_m, 1 \leq m \leq M} \sum_{m=1}^M \mathbb{E}_{\xi_m \sim P_m} [1 - \pi_m(\xi_m)]. \end{aligned}$$

On the other hand, by Lemma 2, there exists an optimal solution to the minimax problem (8), denoted as (P_1^*, \dots, P_M^*) , and the optimal classifier π^* as given in Lemma 1. Note that there exists $1 \leq k^* \leq n$ and weight functions w_1^*, \dots, w_M^* such that

$$\pi_m^{\text{knn}}(\xi; k^*, w^*) = \pi_m^*(\xi), \quad \forall \xi \in \widehat{\Xi}, \quad (15)$$

for example, by taking $k^* = 1$ and $w_m^* = P_m^*$, $1 \leq m \leq M$. This implies that

$$\begin{aligned} & \min_{\substack{w_m: \Xi \times \Xi \rightarrow \mathbb{R}_+, \\ 1 \leq k \leq K}} \max_{P_m \in \mathcal{P}_m, 1 \leq m \leq M} \sum_{m=1}^M \mathbb{E}_{\xi_m \sim P_m} [1 - \pi_m^{\text{knn}}(\xi_m; k, w)] \\ & \leq \max_{P_m \in \mathcal{P}_m, 1 \leq m \leq M} \sum_{m=1}^M \mathbb{E}_{\xi_m \sim P_m} [1 - \pi_m^{\text{knn}}(\xi_m; k^*, w^*)] \\ & = \max_{P_m \in \mathcal{P}_m, 1 \leq m \leq M} \sum_{m=1}^M \mathbb{E}_{\xi_m \sim P_m} [1 - \pi_m^*(\xi_m)] \\ & = \min_{\pi: \widehat{\Xi} \rightarrow \Delta_M} \max_{P_m \in \mathcal{P}_m, 1 \leq m \leq M} \sum_{m=1}^M \mathbb{E}_{\xi_m \sim P_m} [1 - \pi_m(\xi_m)]. \end{aligned}$$

Thereby we have shown that formulations (6) and (8) have identical optimal values. Moreover, by the strong duality results in Theorem 1, we know $(\pi^*; P_1^*, \dots, P_M^*)$ is the saddle point for the formulation (8), and by the above arguments, we see that $(\pi^{\text{knn}}; P_1^*, \dots, P_M^*)$ leads to the same optimal value for formulation (6) as $(\pi^*; P_1^*, \dots, P_M^*)$ for formulation (8). Therefore, we show that π^{knn} is indeed the optimal solution to (6). \square

A.3 Proof of Theorem 3

Proof of Theorem 3. We first show the equivalence between the Lipschitz regularized problem (11) and the minimax problem (8). Denote by v_{Lip} the optimal value of (11) and v_{dual} the optimal value of (10).

Observe that if $\|\pi_m\|_{\text{Lip}} \leq \lambda_m$, then

$$\max_{\xi \in \widehat{\Xi}} \left\{ 1 - \pi_m(\xi) - \lambda_m c(\xi, \widehat{\xi}) \right\} = 1 - \pi_m(\widehat{\xi}), \quad \forall \widehat{\xi} \in \widehat{\Xi}.$$

Therefore, we have

$$\begin{aligned}
v_{\text{dual}} &\leq \min_{\pi: \widehat{\Xi} \rightarrow \Delta_M, (\lambda_m)_{1 \leq m \leq M} \geq 0, \|\pi_m\|_{\text{Lip}} \leq \lambda_m} \left\{ \sum_{m=1}^M \lambda_m \vartheta_m + \mathbb{E}_{\hat{\xi} \sim \widehat{P}_m} \left[\max_{\xi \in \widehat{\Xi}} \left\{ 1 - \pi_m(\xi) - \lambda_m c(\xi, \hat{\xi}) \right\} \right] \right\} \\
&= \min_{\pi: \widehat{\Xi} \rightarrow \Delta_M} \left\{ \sum_{m=1}^M \|\pi_m\|_{\text{Lip}} \vartheta_m + \mathbb{E}_{\hat{\xi} \sim \widehat{P}_m} \left[1 - \pi_m(\hat{\xi}) \right] \right\} \\
&= v_{\text{Lip}}.
\end{aligned}$$

If we can show $v_{\text{dual}} \geq v_{\text{Lip}}$, then we prove the equivalence between (11) and (10), thus the equivalence between (11) and (8).

Let $(\pi^*; \lambda_1^*, \dots, \lambda_M^*)$ be a dual minimizer of problem (10), whose existence is ensured by [Gao & Kleywegt(2016)Gao and Kleywegt].

Define

$$\phi_m(\xi) := \max_{\tilde{\xi} \in \widehat{\Xi}} \left\{ 1 - \pi_m^*(\tilde{\xi}) - \lambda_m^* c(\tilde{\xi}, \xi) \right\}, \quad m = 1, \dots, M.$$

Then it follows that

$$\pi_m^*(\tilde{\xi}) \geq 1 - \lambda_m^* c(\tilde{\xi}, \xi) - \phi_m(\xi), \quad \forall \xi, \tilde{\xi} \in \widehat{\Xi}, \quad m = 1, \dots, M.$$

Define

$$\tilde{\pi}_m(\tilde{\xi}) := \max_{\xi \in \widehat{\Xi}} \{ 1 - \lambda_m^* c(\xi, \tilde{\xi}) - \phi_m(\xi) \}, \quad m = 1, \dots, M.$$

Then by definition, $\|\tilde{\pi}_m\|_{\text{Lip}} \leq \lambda_m^*$. Indeed, for any $\xi, \tilde{\xi} \in \widehat{\Xi}$, there exists a $\xi_0 \in \arg \max_{\xi \in \widehat{\Xi}} \{ 1 - \lambda_m^* c(\hat{\xi}, \xi) - \phi_m(\hat{\xi}) \}$ such that:

$$\begin{aligned}
\tilde{\pi}_m(\xi) - \tilde{\pi}_m(\tilde{\xi}) &= 1 - \lambda_m^* c(\xi_0, \xi) - \phi_m(\xi_0) - \tilde{\pi}_m(\tilde{\xi}) \\
&\leq [1 - \lambda_m^* c(\xi_0, \xi) - \phi_m(\xi_0)] - [1 - \lambda_m^* c(\xi_0, \tilde{\xi}) - \phi_m(\xi_0)] \\
&= \lambda_m^* c(\xi_0, \tilde{\xi}) - \lambda_m^* c(\xi_0, \xi) \\
&\leq \lambda_m^* c(\xi, \tilde{\xi}).
\end{aligned}$$

Furthermore, since $\tilde{\pi}_m(\tilde{\xi}) \geq 1 - \lambda_m^* c(\xi, \tilde{\xi}) - \phi_m(\xi), \forall \xi, \tilde{\xi}$, we have $\phi_m(\xi) \geq 1 - \tilde{\pi}_m(\tilde{\xi}) - \lambda_m^* c(\xi, \tilde{\xi}), \forall \tilde{\xi} \in \widehat{\Xi}$. Hence, we have $\phi_m(\xi) \geq \max_{\tilde{\xi} \in \widehat{\Xi}} \{ 1 - \tilde{\pi}_m(\tilde{\xi}) - \lambda_m^* c(\xi, \tilde{\xi}) \}$. Recall that $(\pi^*; \lambda_1^*, \dots, \lambda_M^*)$ is a dual minimizer of problem (10):

$$v_{\text{dual}} := \sum_{m=1}^M \lambda_m^* \vartheta_m + \mathbb{E}_{\hat{\xi} \sim \widehat{P}_m} \left[\max_{\xi \in \widehat{\Xi}} \left\{ 1 - \pi_m^*(\xi) - \lambda_m^* c(\xi, \hat{\xi}) \right\} \right] = \sum_{m=1}^M \lambda_m^* \vartheta_m + \mathbb{E}_{\hat{\xi} \sim \widehat{P}_m} \left[\phi_m(\hat{\xi}) \right],$$

thus

$$v_{\text{dual}} \geq \sum_{m=1}^M \lambda_m^* \vartheta_m + \mathbb{E}_{\hat{\xi} \sim \widehat{P}_m} \left[\max_{\xi \in \widehat{\Xi}} \left\{ 1 - \tilde{\pi}_m(\xi) - \lambda_m^* c(\xi, \hat{\xi}) \right\} \right] = \sum_{m=1}^M \lambda_m^* \vartheta_m + \mathbb{E}_{\hat{\xi} \sim \widehat{P}_m} \left[1 - \tilde{\pi}_m(\hat{\xi}) \right].$$

Since v_{dual} is the minimum value, this means that if $\tilde{\pi}$ is a feasible solution, then it is also an optimal solution to (10).

Next we verify $\tilde{\pi}$ is a feasible classifier, i.e., it satisfies $0 \leq \tilde{\pi}(\xi) \leq 1$ and $\sum_{m=1}^M \tilde{\pi}_m(\xi) = 1, \forall \xi$. First, by definition, $\pi_m^*(\tilde{\xi}) \geq \tilde{\pi}_m(\tilde{\xi}), \forall \tilde{\xi} \in \hat{\Xi}$, therefore $\tilde{\pi}_m(\tilde{\xi}) \leq 1$ and $\sum_{m=1}^M \tilde{\pi}_m(\tilde{\xi}) \leq 1$. If we are able to show that

$$\sum_{m=1}^M \tilde{\pi}_m(\tilde{\xi}) \geq 1, \quad \forall \tilde{\xi} \in \hat{\Xi}, \quad (16)$$

then we can show $\tilde{\pi}$ is indeed a feasible classifier.

To show (16), first note that if $\pi_m^*(\tilde{\xi}) = 0$, then we have by definition $\tilde{\pi}_m(\tilde{\xi}) = 0$. Moreover, for any $\tilde{\xi} \in \hat{\Xi}$, there is a set $\mathcal{M}_0 \subset \{1, \dots, M\}$ such that for all $m \in \mathcal{M}_0$, $\pi_m^*(\tilde{\xi}) > 0$, and the worst-case distribution P_m^* transports probability mass from $\text{supp } \hat{P}_m$ to $\tilde{\xi}$, which suggests that there exists $\hat{\xi}_m \in \text{supp } \hat{P}_m$ such that

$$\tilde{\xi} \in \arg \max_{\xi \in \hat{\Xi}} \{1 - \pi_m^*(\xi) - \lambda_m^* c(\xi, \hat{\xi}_m)\}.$$

It follows from the definition of ϕ_m that

$$\sum_{m \in \mathcal{M}_0} \phi_m(\hat{\xi}_m) = \sum_{m \in \mathcal{M}_0} \left(1 - \pi_m^*(\tilde{\xi}) - \lambda_m^* c(\tilde{\xi}, \hat{\xi}_m)\right).$$

Meanwhile, by definition of $\tilde{\pi}_m$,

$$\sum_{m \in \mathcal{M}_0} \tilde{\pi}_m(\tilde{\xi}) \geq \sum_{m \in \mathcal{M}_0} \left(1 - \lambda_m^* c(\tilde{\xi}, \hat{\xi}_m) - \phi_m(\hat{\xi}_m)\right) = \sum_{m \in \mathcal{M}_0} \pi_m^*(\tilde{\xi}) = 1.$$

Thereby we have shown (16). The proof is completed by noting that the optimal solution $\tilde{\pi}$ satisfies $\|\tilde{\pi}_m\|_{\text{Lip}} \leq \lambda_m^*$ and thus $v_{\text{dual}} \geq v_{\text{Lip}}$. Combine with the previous result that $v_{\text{dual}} \leq v_{\text{Lip}}$, we have shown $v_{\text{dual}} = v_{\text{Lip}}$ and the proof is completed. \square

A.4 Proof of Corollary 1

Proof. Using the proof of Theorem 3, there exists a classifier $\tilde{\pi}$ that satisfies $\|\tilde{\pi}_m\|_{\text{Lip}} \leq \lambda_m^*$ which is the optimal solution to problem (11) and (10), and thus is an optimal robust classifier to problem (8). Moreover, based on the proof of Theorem 2, we know that the set of weighted k -NN classifiers is exhaustive and there exist weight functions $w^* = \{w_1^*, \dots, w_M^*\}$ such that $\pi^{\text{knn}}(\cdot; 1, w^*)$ is equivalent to $\tilde{\pi}$. Therefore, $\pi^{\text{knn}}(\cdot; 1, w^*)$ is an optimal solution satisfying

$$\|\pi_m^{\text{knn}}(\cdot; 1, w^*)\|_{\text{Lip}} \leq \lambda_m^*, \quad m = 1, \dots, M.$$

It was shown in [von Luxburg & Bousquet(2004)von Luxburg and Bousquet] that the generalization gap of Lipschitz classifiers is bounded by the corresponding Rademacher complexity. In our setting, a direct consequence of [von Luxburg & Bousquet(2004)von Luxburg and Bousquet] shows that the generalization gap of $\pi^{\text{knn}}(\cdot; 1, w^*)$ is controlled by $\max_{1 \leq m \leq M} \lambda_m^* \cdot \mathfrak{R}_n(\text{Lip}(\Xi))$, where $\max_{1 \leq m \leq M} \lambda_m^*$ denotes the maximum Lipschitz norm of the classifier $\{\pi_m^{\text{knn}}\}_m$ and $\mathfrak{R}_n(\text{Lip}(\Xi))$ denotes the Rademacher complexity of the class of 1-Lipshitz functions on the sample space Ξ . Moreover, note that the optimal dual minimizer λ_m^* satisfies $\lambda_m^* \leq 1/\vartheta_m, \forall m$. Indeed, if $\lambda_m^* > 1/\vartheta_m$, then the objective value in the m -th term in (10) is larger than 1, which is clearly not optimal. Thereby we have $\max_{1 \leq m \leq M} \lambda_m^* = \frac{1}{\min_{1 \leq m \leq M} \vartheta_m}$ and we complete the proof. \square

B Memory-efficient implementation of Dr.k-NN in data-intensive scenario

For the sake of completeness, we extend our algorithm to non-few-training-sample setting. This can be particularly useful for the general classification problem with an arbitrary size of training set. In fact, k -NN methods notoriously suffer from computational inefficiency if the number of labeled samples n is large, since it has to store and search through the entire training set [Goldberger et al.(2005)Goldberger, Hinton, Roweis, and Salakhutdinov].

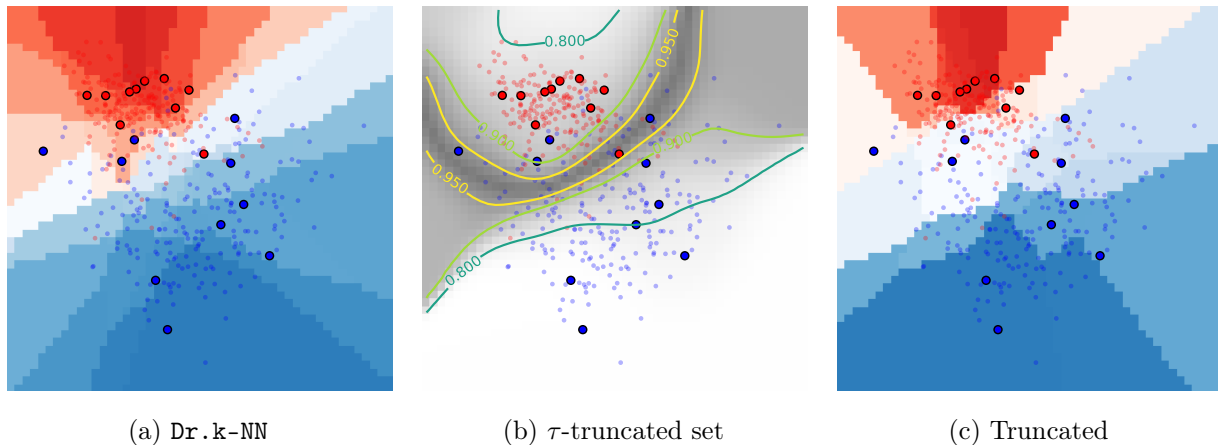


Figure 6: An example of the truncated Dr.k-NN using MNIST (digit 4 (red) and 9 (blue)). Big dots represent training samples and small dots represent query samples. (a) shows the decision made by Dr.k-NN; (c) shows the decision by the truncated Dr.k-NN with truncation level $\tau = 0.9$; (b) shows τ -truncated regions with $\tau = 0.95, 0.9, 0.8$. Big dots between the lines are selected training samples under different τ . The depth of the shaded area shows the level of samples entropy.

The main idea is to only keep the training samples that are important in deciding the decision boundary based on the maximum entropy principle [Cover & Thomas(2006)Cover and Thomas]. As a measure of importance, we choose the samples with the largest entropy across all categories, based on the intuition that the samples with higher entropy has larger uncertainty and will be more useful for classification purposes since they tend to lie on the decision boundary. The entropy of a sample is defined as follows. Consider a random variable which takes value m with probability π_m , $\sum_{i=1}^M \pi_m = 1$; then the entropy of this random variable is define as

$$H(\pi_1, \dots, \pi_M) = - \sum_{m=1}^M \pi_m \log \pi_m.$$

As a simple example, for Bernoulli random variable (which can represent, e.g., the outcome for flipping a coin with bias p), the entropy function is $H(p) = -p \log p - (1 - p) \log(1 - p)$, and it is a concave function achieving the maximum at $p^* = 1/2$, which means that the fair-coin has the maximum entropy; this is intuitive as indeed the outcome of a fair coin toss is the most difficult to predict. Now we use this entropy to define the “uncertainty” associated with each training points. With a little abuse of notation, define

$$H(\hat{\xi}) := H(\pi_1(\hat{\xi}), \dots, \pi_M(\hat{\xi})).$$

Denote the minimal and maximal entropy of all the training points as

$$H_{\min} = \min\{H(\hat{\xi}), \hat{\xi} \in \hat{\Xi}\}, \quad H_{\max} = \max\{H(\hat{\xi}), \hat{\xi} \in \hat{\Xi}\}.$$

Define the τ -truncated training set as

$$\tilde{\Xi} = \{\hat{\xi} \in \hat{\Xi} : (H(\hat{\xi}) - H_{\min}) / (H_{\max} - H_{\min}) \geq \tau\}, \forall \tau \in [0, 1].$$

The truncated **Dr.k**-NN is obtained similarly as Step 2 of **Dr.k**-NN by restricting the training set $\hat{\Xi}$ only to the samples in $\tilde{\Xi}$ (samples with larger entropy). Figure 6 reveals that the most informative samples usually lie in between categories. We can see that a truncated **Dr.k**-NN classifier with $\tau = 0.9$ only uses 20% samples with little performance loss. More experimental details is presented in Section 5.

C Comparison to kernel smoothing

Figure 7 and Figure 8 present a comparison of the results using Dr.k-NN and the kernel smoothing defined in (13). The results suggest that the performance of Dr.k-NN is insensitive to the choice of k , while the performance of the kernel smoothing is heavily depended on the choice of h .

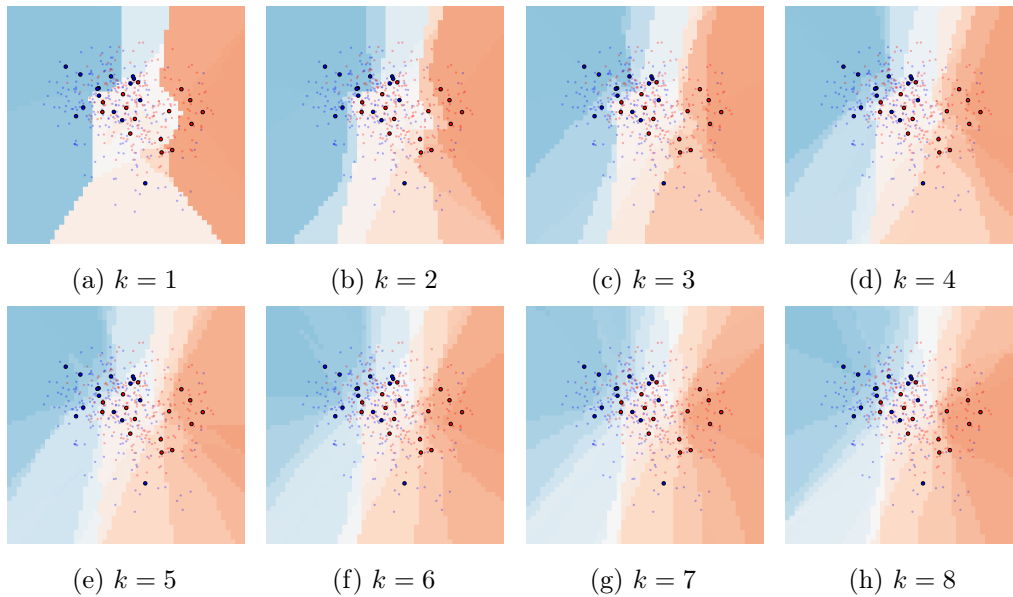


Figure 7: Dr.k-NN with different k .

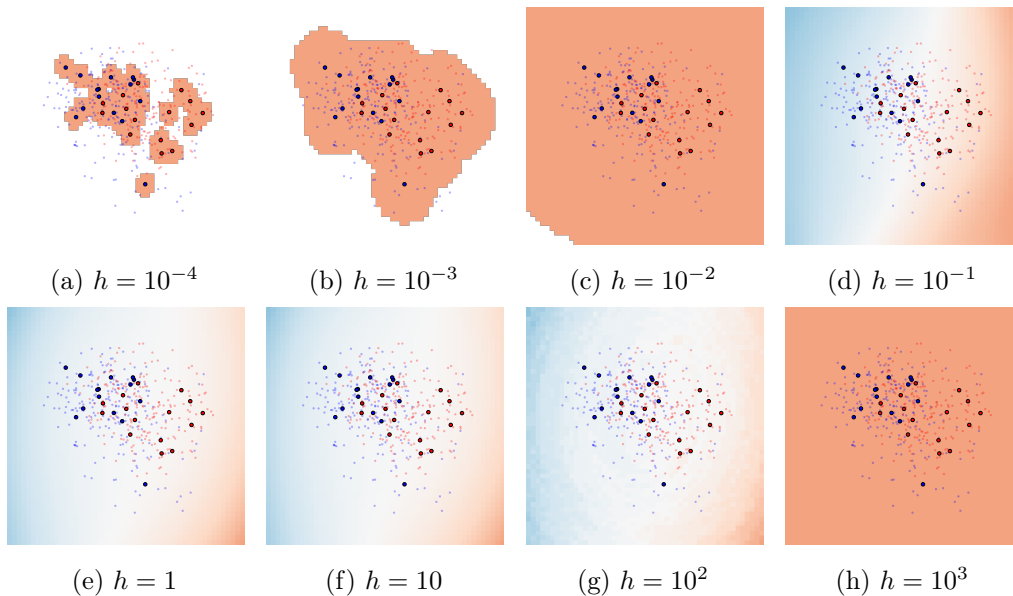


Figure 8: Kernel smoothing with different bandwidth h .

D Real data examples for COVID-19 CT

Figure 9 and Figure 10 show 16 real CT images collected from patients who have been diagnosed with COVID-19 and other diseases (non-COVID-19), respectively.

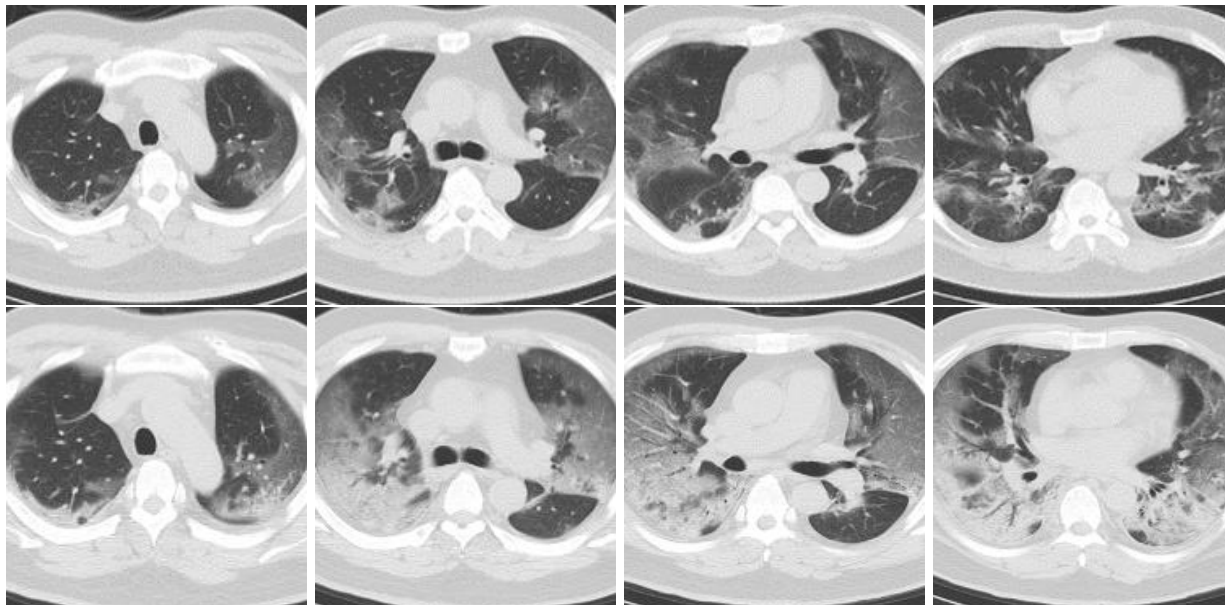


Figure 9: COVID-19 CT images.

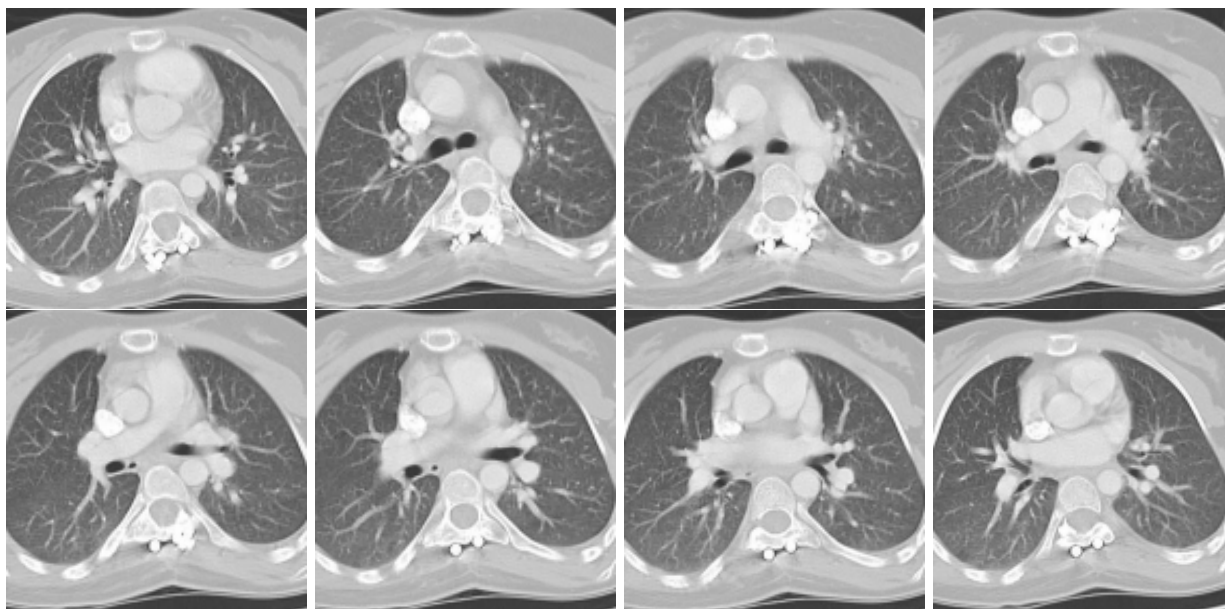


Figure 10: Non-COVID-19 CT images.